Porosity Effects on Catalytic Char Oxidation

Part I: A Catalyst Deposition Model

Six char samples generated from two coals were impregnated by solutions with different concentrations of Na_2CO_3 and/or K_2CO_3. The catalyst solution penetration was studied, the catalyst uptake was measured, and the effects of impregnation on the char pore structure were determined experimentally. The results indicate that the impregnated catalysts reside only on particle exteriors without significant penetration. The overall rate of reaction is therefore the combination of catalytic reaction on particle exteriors and noncatalytic reaction on the pore surfaces inside the particle. A kinetic model is presented that takes these findings into account.

J. L. SU and
D. D. PERLMUTTER

Department of Chemical Engineering
University of Pennsylvania
Philadelphia, PA 19104

SCOPE

Six char samples generated from two coals were impregnated by solutions containing different concentrations of Na_2CO_3 and/or K_2CO_3. The effects of catalyst impregnation on the char pore structure were examined by CO_2 adsorption and mercury porosimetry. The catalyst uptakes were determined by atomic absorption. Pycnometry tests were also conducted to determine the degree of catalyst penetration during impregnation. Catalyzed and uncatalyzed samples were examined under a scanning electron microscope at both unreacted and partially reacted stages. The experimental results were used to formulate a kinetic model that accounts for the several findings.

CONCLUSIONS AND SIGNIFICANCE

The experimental work of this study focused on the degree of catalyst solution penetration that occurs during impregnation of chars. The catalyst uptake was determined as well as the effects of impregnation on the char pore structure. The impregnating solution was found unable to penetrate into the interior pore structure of a char. The deposited catalysts resided mainly on particle exteriors without affecting the pore structure. As a consequence, rapid catalytic reaction occurs on a char's exterior surfaces, reducing particle size, while a slower noncatalytic reaction occurs simultaneously inside the pore structures. The observed reaction rate is then the combination of the contributions from catalytic and noncatalytic mechanisms.

From such a physical picture a model was developed for reaction kinetics of catalytic gasification. The model produces an expectation that the enhanced reactivity would be more significant at low levels of conversion, and predicts that the overall rate would decrease to that of the noncatalytic reaction at high conversion. The contributions to the overall reaction rate of catalytic and noncatalytic steps are discussed.

INTRODUCTION

The effects of certain inorganics, particularly alkali carbonates, in enhancing various char gasification reactions were recognized early in this century by Taylor and Neville (1921). The interest in this catalysis has been renewed with the increased emphasis on coal gasification processes (Hirsch et al., 1982). The addition of the catalyst not only increases the char gasification rate, thus permitting operation at lower temperatures, but also inhibits the undesirable swelling and agglomeration of caking coals (Vargas, 1982).

TABLE 1. CHEMICAL AND PHYSICAL PROPERTIES OF COAL SAMPLES

A. Chemical Composition (Spackman, 1976)

Coal Sample	Rank (Location)	Ultimate Analysis Carbon %	H %	N %	O %	S %	Proximate Analysis Ash %	Volatile Matter %	Water Content %
PSOC-80	Anthracite (Pennsylvania)	78.18	2.25	0.66	4.42	0.55	13.94	5.77	2.51
PSOC-4	HVA bituminous (Kentucky)	82.10	5.67	1.52	7.78	0.86	2.07	37.51	2.48

B. Pore Structure (Gan et al., 1972)

Coal Sample	Pore Volumes, cm^3/g >300Å	12 to 300Å	<12Å	Total
PSOC-80	0.009	0.010	0.057	0.076
PSOC-4	0.017	0.000	0.016	0.033

The extensive literature that exists on the subjects of kinetics and mechanisms in catalytic gasification has been reviewed by, among others, Walker et al. (1966), Johnson (1976), Prasher (1979), Wen (1980), and McKee (1981, 1983). It has been common to correlate the measured overall reaction rate with the total amount of added catalyst (Patrick and Shaw, 1975; Verra and Bell, 1978; Lang and Neavel, 1982; Walker et al., 1983; Spiro et al., 1983; Huhn et al., 1983). Such an approach is in effect a homogeneous approximation to a heterogeneous process, since it does not account for changes in the solid physical properties such as porosity, surface area, and particle size. Furthermore, it should be noted that the catalyst deposition is not necessarily uniform over the reactive char surface, especially if the catalyst solution does not penetrate deeply into the pores of a char particle during the impregnation treatment. This nonuniform deposition will produce an overall effect which will be a combination of catalytic and noncatalytic rates.

In the work reported in this study, experiments focused on the catalyst solution penetration during impregnation and the catalyst uptake, as well as on the effects of impregnation on the char pore structure. The results were used to formulate a kinetic model that takes these findings into account.

EXPERIMENTAL

Char Preparation

Two types of coals from the DOE-Penn State Coal Bank were used in this study, chosen for their contrasting physical and chemical properties, notably volatile matter, ash content, and pore size distribution. The coals are identified by code numbers: PSOC-80, a high-rank anthracite; and PSOC-4, a lower rank high-volatile bituminous coal. The proximate and ultimate analyses as well as pore structure information for these coals are given in Table 1.

Chars were prepared by pyrolyzing each coal under nitrogen flow. Coal samples of approximately one gram and average particle diameter of 250 micron were placed in a ceramic boat in quartz tube and heated in a furnace at a controlled rate to a preset final pyrolysis temperature. Thereafter the samples were allowed to cool to room temperature under the same nitrogen flow. Details are given in Table 2 on the heating program for each of six char preparations.

TABLE 2. CHAR SAMPLES AND THEIR PREPARATION CONDITIONS

Char Sample	Parent Coal	Pyrolysis Heating Rate, °C/min	Final Pyrolysis Temp., °C
A	PSOC-80	10	600
B	PSOC-4	10	600
C	PSOC-4	10	750
D	PSOC-4	10	950
E	PSOC-4	5	600
F	PSOC-4	1	600

Catalyst Impregnation

Inorganics were deposited on the chars by a wet impregnation method of Vargas (1982) that uses a flow system to circulate catalyst solution of a desired concentration through a char sample bed. The wet impregnation method is preferred because it provides uniform catalyst-particle contact, and the flow system reduces possible uneven catalyst deposition for those lighter char particles that might otherwise float on the solution surface. Upon completion of a one-hour impregnation, the sample was removed from the bed and vacuum dried overnight at room temperature. The dried impregnated samples were then further sieved to remove excess inorganics that might exist in interstices between char particles, and stored in a dessicator under vacuum.

Pore Structure

A Micromeritic model 910 mercury porosimeter was used to study the macropore structure of chars. The instrument provides mercury penetration pressure up to 50,000 psi (344.5 MPa), corresponding to a minimum measurable pore radius of 17 Å (1.7 nm). Pores of smaller size were analyzed by CO_2 adsorption at 273 K using a Quantasorb Sorption System (Quantachrome Co., as described in detail by Su (1983). The isotherms obtained were interpreted according to the Dubinin-Polyani equation (Su, 1983).

Pycnometry

A specially made sample cell attached to the Quantasorb system, but volume-calibrated at the factory, allowed measurement of true powder density. After successive nitrogen fills and helium purges, the true volume of a 5g weighed sample, excluding pore volume, was obtained as the difference between cell volume and the nitrogen volume swept out of the sample cell.

Determination of Catalyst Uptake

The exact amount of catalyst uptake was determined by an atomic absorption technique. The sample preparation procedures followed those suggested by Hartstein et al. (1973), which dissolve the impregnated chars in fuming nitric acid and hydrofluoric acid at 423 K. The details of sample preparation and atomic absorption spectrophotometry are available elsewhere (Su, 1983).

Scanning Electron Microscopy

Deposited catalysts and their effects during gasification were observed and photographed through a Philips model 500 scanning electron micro-

TABLE 3. PORE STRUCTURE PARAMETERS FOR UNREACTED CHAR SAMPLES

Sample	True Density g/cm³	Macropores Volume cm³/g	Macropores Surface m²/g	Micropores Volume cm³/g	Micropores Surface m²/g	Total Pores Volume cm³/g	Total Pores Surface m²/g	Total Pores Pore Length m/g	Porosity	Structural Parameter ψ
A	1.41	0.025	1.8	0.074	201	0.099	203	4.69×10^{10}	0.12	10.14
B	1.42	0.187	12.3	0.098	275	0.285	287	6.40×10^{10}	0.29	6.88
C	1.61	0.113	6.3	0.085	251	0.198	257	6.13×10^{10}	0.24	7.24
D	1.82	0.080	5.9	0.054	143	0.134	149	3.16×10^{10}	0.20	9.83
E	1.54	0.152	13.4	0.076	222	0.228	235	5.37×10^{10}	0.26	7.93
F	1.63	0.051	4.0	0.059	166	0.110	170	3.85×10^{10}	0.15	9.68

scope (SEM) fitted with an attachment for Polaroid instant photography.

RESULTS AND DISCUSSION

Effect of Impregnation on Pore Structure

The pore structures of the unimpregnated char samples *A* to *F* were obtained by combining mercury penetration porosimetry with CO_2 adsorption at 273 K. These results are listed in Table 3, together with true densities measured by pycnometry (excluding pore volumes). The tabulated porosities are also included in Table 3, computed from the total pore volume V_T and the true particle density ρ_t by:

$$\epsilon = \frac{V_t}{V_T + (1/\rho_t)} \tag{1}$$

Pores with radii larger than 1.5 micron were not included in these calculations because their volumes were experimentally indistinguishable from the volumes of particle interstices.

Since the catalyst-enhanced reactivity of char may be due to either the chemical catalytic effect or the physical structural change, or both, it is important to determine whether the pore structure of a char is altered by the impregnation treatment. For this purpose CO_2-adsorption isotherms were determined for chars before and after treatment. The results for samples *A* and *B* treated with different concentrations of Na_2CO_3 and K_2CO_3 solutions are shown in Figures 1 and 2 on the coordinates suggested by the Dubinin-Polyani equation, showing clearly that the adsorption capacities of chars, and therefore their surface areas, were not affected by the impregnation.

The effects of impregnation on macro- and mesopore structures were also studied. As shown in Figure 3, treatment with Na_2CO_3 solution had no effect on mercury porosimetry results for either sample *A* or *B*. When treated with K_2CO_3 solutions, however, the macropore volume of sample *B* clearly decreased with increase in K_2CO_3 concentration, as presented in Figure 4. This is probably an indication of pore blockage by the catalyst. Such decreases in macropore volume are not expected to have any significant effect on the subsequent gasification kinetics because the contribution by the macropores to the overall reactive surface area is negligible.

It can therefore be concluded that the pore structures remain largely intact except for some blocking, but this finding must be limited to the char samples used in this study, since results by other

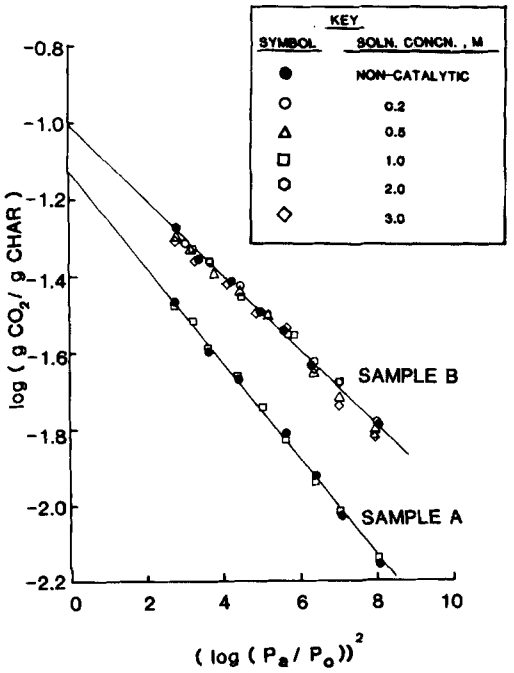

Figure 1. CO_2 adsorption capacities of unreacted char samples *A* and *B* treated with different concentrations of Na_2CO_3 solution.

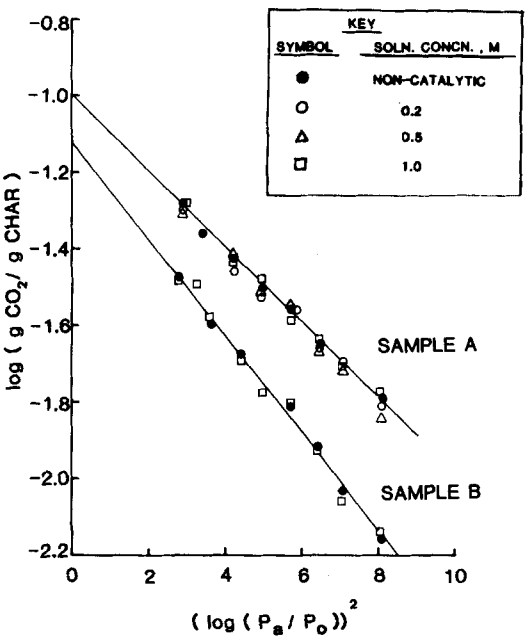

Figure 2. CO_2 adsorption capacities of unreacted char samples *A* and *B* treated with different concentrations of K_2CO_3 solution.

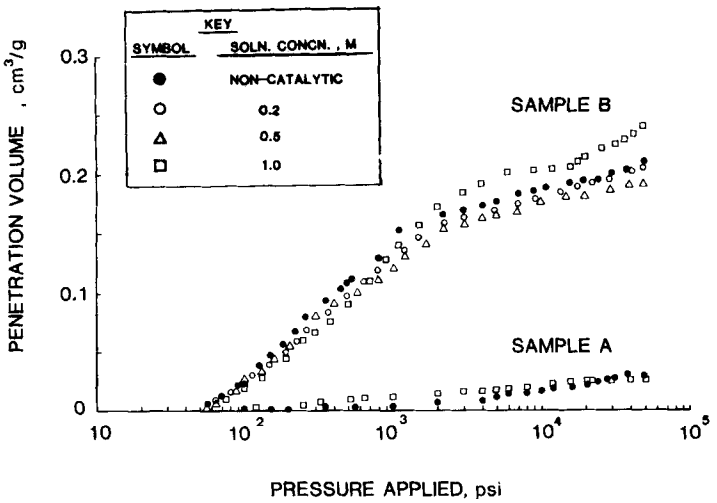

Figure 3. Mercury porosimetry results of unreacted char samples *A* and *B* treated with different concentrations of Na_2CO_3 solution.

workers vary widely in this regard. Wigmans et al. (1983c) reported that no significant differences in surface areas were found between K_2CO_3 catalyzed and uncatalyzed activated carbons, even after further devolatilization. Senkan and Fuller (1979) showed on the other hand that CO_2 and N_2 sorption capacities of Wyodak coal decreased significantly after an NaOH treatment. A more complete study by Trupathi and Ramachandran (1982) showed that the micropore structure of activated carbons was not affected by impregnating with 2.08% of copper. Higher copper concentration, however, caused a steady decrease of micropore volumes. On the contrary, Patrick and Shaw (1972) reported increases of macropore volumes of cokes with increases of Na_2CO_3 concentration. It is apparent from these results that the effects of catalyst impregnation on the pore structure of chars depend strongly on the specific samples and impregnation techniques used.

Amount of Catalyst Uptake

Whether it is accomplished by dry physical means such as bulk mixing or ball milling, or by solution soaking and drying, the purpose of impregnation is to spread catalyst over the char surface area. A catalytic activity study based on a total amount of added catalyst can be misleading, however, if a large portion of the catalyst added in this fashion exists only in char particle interstices without direct contact on the char surface, for it then does not contribute to the increased reactivities.

In this study the amount of catalyst uptake was determined by atomic absorption spectrophotometry. The impregnated, dried samples were further sieved before atomic absorption tests to remove inorganics that might exist in interstices between char particles. The results for various chars treated by different concentrations of Na_2CO_3 or K_2CO_3 aqueous solutions for one hour are shown in Table 4. The Na and K naturally contained in these char samples are around 0.07 and 0.04 wt%, respectively. The Na and K contents of the catalyst-impregnated chars are substantially higher. Increasing catalyst solution concentration from 0.2 M to 1.0 M causes significant uptake increase; however, the results on sample *B* show that higher concentrations of 2.0 M or 3.0 M do not further increase the uptake, indicating a saturation effect. Treated by the same concentration of catalyst solution (1.0 M), the char generated from anthracite (sample *A*) exhibited considerably less

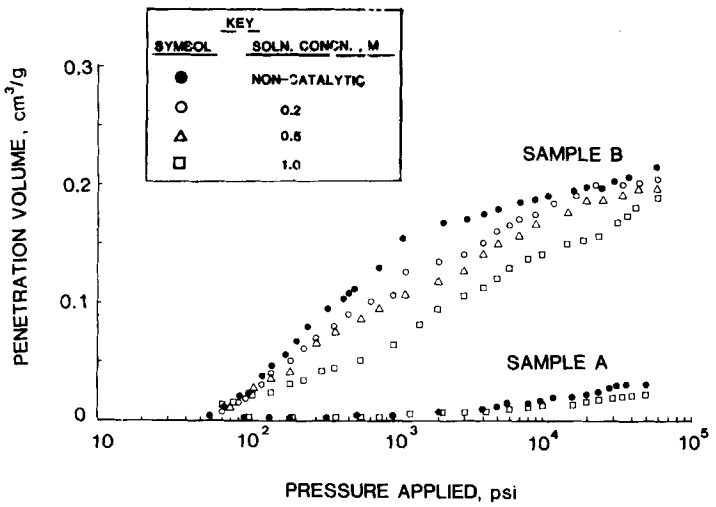

Figure 4. Mercury porosimetry results of unreacted char samples *A* and *B* treated with different concentrations of K_2CO_3 solution.

TABLE 4. Na AND K CONTENT (IN WT. %) OF Na_2CO_3 AND K_2CO_3 IMPREGNATED CHAR SAMPLES

Catalyst	Sample	Concentration of Impregnating Solution: Non-catalytic	0.2 M	0.5 M	1 M	2 M	3 M
Na_2CO_3	A	0.08	—	—	0.19	—	—
	B	0.06	0.21	1.00	1.55	1.64	1.51
	C	0.07	0.39	0.52	1.25	—	—
	D	0.09	0.39	0.55	0.78	—	—
	E	0.07	0.47	0.89	1.01	—	—
	F	0.07	0.50	0.77	0.81	—	—
K_2CO_3	A	0.04	—	—	0.35	—	—
	B	0.03	0.32	0.73	1.23	—	—

catalyst uptake then those chars prepared from the chemically different bituminous coal.

Repetitive runs on three specimens taken from the same batch of the impregnated chars gave catalyst uptake results within ±16%, but mostly within 10%. The same chars impregnated in different batches showed larger variation in catalyst uptake, in some cases as large as 30%. For consistency the impregnated chars prepared in the first batch were used in the subsequent reactivity studies. Changing impregnation time in the range of 15 min to 3 h was found to have no effect on the amount of catalyst uptake.

Catalyst Penetration

Solution treating is expected to spread catalyst more uniformly than dry mixing, but whether the catalyst can penetrate into pore structures depends on the specific conditions of solid and solution. The solution treating process can be either liquid diffusion through a porous medium or simply a porous-solid wetting problem, depending on whether char particles are originally wet or dry. In the former case, the degree of catalyst deposition is affected by impregnation time and effective diffusivity (Prasher, 1979), while in the latter case, such as in this study as well as in most of the prior works (Veraa and Bell, 1978; Wigmans et al., 1983b; Yuh and Wolf, 1983), the wettability of catalyst solution on char surface is a controlling parameter.

The wettability of catalyst solution on coal or char surfaces has not been studied in depth, probably due to the heterogeneity and diversity of coal substances. The contact angles between water and graphite are reported to be in the ranges of 50 to 80° (Schrader, 1975). The contact angles between water and several saturated solid hydrocarbons such as cycloparaffins with 15, 16, and 17 $-CH_2-$ groups are around 105° (Adam and Elliott, 1952). The chemical structure of char suggests that its contact angle with water could fall between these ranges. Thus, depending on the specific char and catalyst, the aqueous solution can be either a wetting or a nonwetting liquid, with respect to char. Indeed both cases have been reported. Ingles (1957) reported that water could not wet the chars he studied. On the other hand, Wigmans et al. (1983c) measured the pore volume of activated carbons pycnometrically by using water as the penetrating liquid, suggesting that water is a wetting material to activated carbons. Senkan and Fuller (1979) also reported that the internal surface properties of coal were significantly changed after treatment by NaOH solution, indicating that internal pore structure was accessible to the solution used. It should be noted however that even a wetting fluid will not penetrate fully into pores unless the gas originally in the pore volume is removed. An example was reported by Haggin (1982) in one of the Exxon studies which showed that dried coals had lower nickle uptake tan wet-as-received coals when both were exposed to an aqueous solution of nickle sulfate.

A set of experiments was conducted to determine whether catalyst solution was able to penetrate the pore structures of the chars under study here. For a given amount of weighed char, the bulk solid volume V_b and true solid volume (excluding pore volume) V_t can be calculated from porosity and pycnometry data (Table 3). When immersed in a fixed volume of 1 M catalyst solution V_s, the total volume of char and catalyst solution will be $(V_t + V_s)$, if solution penetrates into the pores, or $(V_b + V_s)$ if it does not. As shown in Table 5, the experimental results gave total volumes that exceeded $(V_b + V_s)$ for all six chars tested, indicating that catalyst solution does not penetrate into the pore structure of these chars. The calclated V_b values may be slightly low because the porosities used in the calculation do not account for pores with diameter larger than 3 micron.

Further confirmation of this finding can be obtained from a comparison of char and solution densities. Since the true density of a char is in the range of 1.4 to 1.9 g/cm³ (Table 3), whereas the solution densities of 1 M Na_2CO_3 and K_2CO_3 are 1.11 and 1.14 g/cm³ respectively, the char particles would be expected to drop to the bottom of the liquid phase if catalyst solution penetrated and

TABLE 5. EXPERIMENTAL RESULTS ON CATALYST PENETRATION

Sample	Sample Weight (g)	True Solid Vol. Calc. V_t (mL)	Bulk Solid Vol. Calc. V_b (mL)	Vol. of Solution Used V_s (mL)	$V_t + V_s$ (mL)	$V_b + V_s$ (mL)	Total Solid & Solution Volume Meas. mL: in Na_2CO_3	Total Solid & Solution Volume Meas. mL: in K_2CO_3	Apparent Solid Density Calc. g/mL: in Na_2CO_3	Apparent Solid Density Calc. g/mL: in K_2CO_3
A	5.0	3.54	4.02	5.0	8.54	9.02	9.23	9.31	1.18	1.16
B	5.0	3.54	4.96	5.0	8.52	9.96	10.02	9.84	1.00	1.03
C	5.0	3.11	4.09	5.0	8.11	9.09	10.01	9.48	1.00	1.12
D	5.0	2.75	3.44	5.0	7.75	8.44	9.72	9.06	1.06	1.23
E	5.0	3.25	4.39	5.0	8.25	9.35	9.85	9.77	1.03	1.05
F	5.0	3.07	3.61	5.0	8.07	8.61	9.17	9.24	1.20	1.18

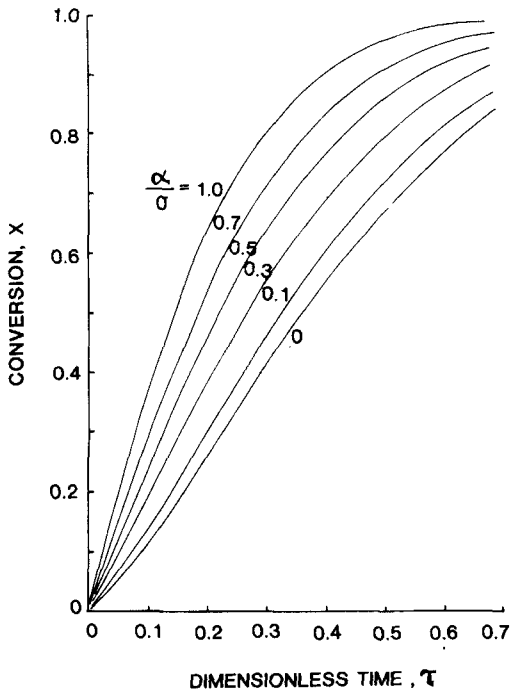

Figure 5. Change of conversion with time for catalytic gasification; parameter $\psi = 10$.

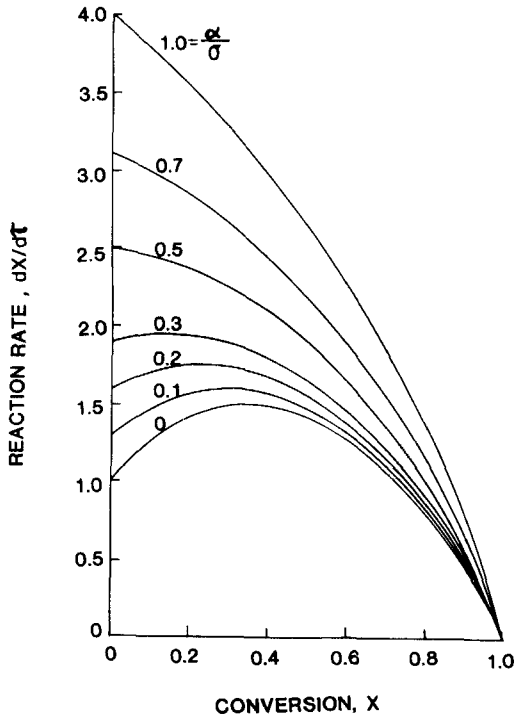

Figure 6. Change of reaction rate with conversion for catalytic gasification; parameter $\psi = 10$.

occupied pore volumes. The opposite was observed during these experiments except for sample *A*: particles partly floated and were partly submerged in solution, indicating an average apparent density very close to 1.1 g/cm^3, consistent with values calculated from experiments (last column of Table 5). The lack of significant penetration is thus directly visible. Therefore it can be concluded that the impregnated catalyst resides only on particle exteriors without penetrating into pore structures. This agrees also with the prior observations that the time of the catalyst treatment has no effect on the catalyst uptake, and that the internal pore structures of chars were not affected by the catalyst impregnation. This finding also helps explain why the method of impregnation, whether by bulk mixing, ball milling, solution soaking, or ion exchange, is sometimes reported to have little effect on gasification rate (Hirsch et al., 1982).

Electron Microscopy

The pattern described above for catalytic gasifications was also observed directly under a scanning electron microscope by examining partially reacted char samples *A* (anthracite) and *B* (bituminous) at different levels of conversion. For samples reacted in air at 673 K without catalyst impregnation, particle size was found to remain intact even at very high levels of conversion. The entire particle did however become more porous and fragile as reaction proceeded, consistent with the picture that gasification was negligible on the particle exteriors and took place mainly inside the particle on the pore surfaces.

In contrst, a significant portion of catalytic gasification took place at particle exteriors where catalyst is present, and surfaces were seriously etched at the catalyst-char contact points, increasing in severity with conversion. There were also fewer cracks on particle exteriors as compared to the noncatalytic reactions at the same conversion levels, indicating that reaction inside the particle occurred to a lesser extent.

MODELING FOR THE KINETIC CONTROL REGIME

Following the arguments and evidence presented above, the overall catalytic oxidation kinetics may be modeled as a combination of contributions from catalytic reaction on particle exteriors and noncatalytic reaction on the pore surfaces.

The fractional conversion of a spherical porous solid particle can be expressed in terms of both porosity and radius by:

$$X = 1 - \left(\frac{1-\epsilon}{1-\epsilon_o}\right)\left(\frac{R}{R_o}\right)^3 \tag{2}$$

The particle exterior reacts at the enhanced catalytic rate:

$$dR/dt = -k_c C_o^m \tag{3}$$

which integrates over the range $0 \leq t \leq (R_o/k_c C_o^m)$ to give

$$R = R_o - k_c C_o^m t \tag{4}$$

The particle interiors react at a noncatalytic rate that increases the particle porosity. According to Bhatia and Perlmutter (1980) this increase in solid porosity can be expressed for the kinetic control regime in the form:

$$\frac{1-\epsilon}{1-\epsilon_o} = \exp[-\tau(1 + \psi\tau/4)] \tag{5}$$

where

$$\tau = \frac{k_s C_o^n t S_o}{1-\epsilon_o} \tag{6}$$

and

$$\psi = \frac{4\pi L_o(1-\epsilon_o)}{S_o^2} \tag{7}$$

Since the pore length, surface, and porosity called for in Eq. 7 can all be computed from the experimentally measured pore volume distribution of the solid before reaction (Bhatia and Perlmutter,

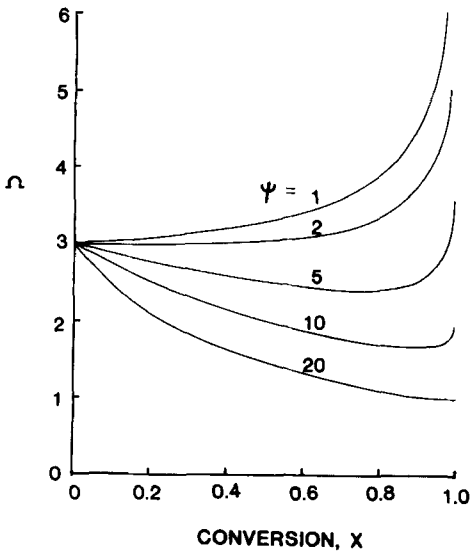

Figure 7. Effect of conversion on ratio of catalytic to noncatalytic contributions to overall reaction rate at different values of ψ; parameter $\alpha/\sigma = 1.0$.

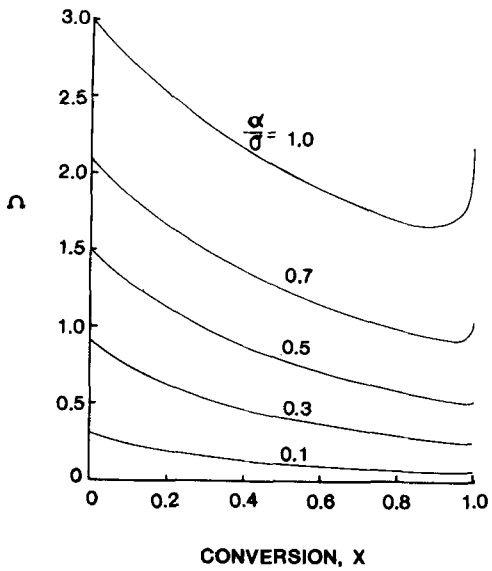

Figure 8. Effect of conversion on ratio of catalytic to noncatalytic contribution to overall reaction rate at different values of α/σ; parameter $\psi = 10$.

1980), the values of ψ for char samples A to F are also listed in Table 3. It should be noted that the needed bulk solid density $\rho_b = \rho_t/(1-\epsilon_o)$.

The ratio of the enhanced intrinsic catalytic rate to the noncatalytic rate may be defined by:

$$\alpha = k_c C_o^m / k_s C_o^n \tag{8}$$

where both numerator and denominator have identical units to describe the intrinsic rate of carbon gasification in terms of exterior particle size reduction or internal pore size enlargement, respectively. If both catalytic and noncatalytic reactions have the same orders of reaction, $m = n$, and α is the ratio of catalytic to noncatalytic rate constants. Combining Eqs. 12, 4, 5, and 8 gives

$$X = 1 - \exp[-\tau(1 + \psi\tau/4)]\left[1 - \frac{\alpha}{\sigma}\tau\right]^3 \tag{9}$$

where σ is a particle size parameter.

The relative catalytic activity may be affected by conversion. As particle size and exterior surface shrink due to catalytic reaction, the concentration of the catalyst per unit surface and therefore the value of α may increase if all the originally deposited catalyst accumulates on the shrinking surface. On the other hand, as char is gasified the ash formed can reduce the contacts between the catalyst and freshly exposed carbon surface, thus decreasing the value of α. These opposite effects may result in a virtually constant value of α over a wide range of conversions, a value that decreases only at very high conversion levels where the loss of catalyst-carbon contacts predominates. A similar argument was presented by Walker et al. (1966) in discussing the possibility of impurities accumulation in noncatalytic carbon gasifications; they expected that the number of contact points between a mixture of impurity and carbon particles would not be greatly affected by conversion. The actual trends in a particular case must be established by experiments.

Assuming for convenience a constant value of α, differentiation of Eq. 9 results in the overall catalytic gasification rate:

$$\frac{dX}{d\tau} = \left[3\frac{\alpha}{\sigma} + \left(1 + \frac{\psi}{2}\tau\right)\left(1 - \frac{\alpha}{\sigma}\tau\right)\right] \times \left(1 - \frac{\alpha}{\sigma}\tau\right)^2 \exp[-\tau(1 + \psi\tau/4)] \tag{10}$$

By combining Eqs. 9 and 10 the overall gasification rate can be further reduced to:

$$\frac{dX}{d\tau} = (1 - X)\left[\left(\frac{3\frac{\alpha}{\sigma}}{1 - \frac{\alpha}{\sigma}\tau}\right) + \left(1 + \frac{\psi}{2}\tau\right)\right] \tag{11}$$

and, since the bracketed terms in Eq. 11 arise from the contributions of the catalytic and noncatalytic reactions, respectively, the ratio of the two rates can be written as

$$\Omega = \frac{3\frac{\alpha}{\sigma}}{\left(1 + \frac{\psi}{2}\tau\right)\left(1 - \frac{\alpha}{\sigma}\tau\right)} \tag{12}$$

PREDICTED TRENDS

The conversion-time behavior predicted for catalytic gasification by Eq. 9 is shown in Figure 5 for $\psi = 10$. Corresponding rate-conversion curves are shown in Figure 6, obtained from the combination of Eqs. 9 and 11, also using the α/σ ratio as a parameter. In comparison to the noncatalytic rate $\alpha/\sigma = 0$, the enhanced reactivity is more significant at low levels of conversion, and the overall rate decreases to that of the noncatalytic reaction at high conversion. Such trends were reported by Otto and Shelef (1976).

Figure 7, obtained from the combination of Eqs. 9 and 12 for various ψ values at $\alpha/\sigma = 1.0$, shows the changes of Ω with conversion. The catalytic rate decreases with conversion monotonically because of the continuous reduction of particle size. The noncatalytic rate, which is directly proportional to the internal surface area developed, can increase through a maximum or decrease monotonically, depending on whether the pore structure parameter ψ is larger or smaller than 2 (Bhatia and Perlmutter, 1980). As a result, Ω decreases over a wide range of conversions for $\psi > 2$, but increases with conversion monotonically for $\sigma \leq 2$. The effects of conversion on Ω are shown in Figure 8 for $\psi = 10$. It can been seen

that the catalytic contribution to overall rate is minimal at high conversions if the initial catalyst uptake is low.

ACKNOWLEDGMENT

This research was funded by the U.S. Department of Energy Fossil Research Program under Contract No. EX-76-S-01-2450.

NOTATION

C_o = ambient concentration of gas reactant, mol/m^3
k_c = catalytic rate constant for char surface reaction, in units that give m/s for $k_c C_o^m$
k_s = noncatalytic rate constant for char surface reaction, in units that give m/s for $k_s C_o^n$
L_o = total pore length per unit volume of unreacted particle, m/m^3
m = reaction order for catalytic reaction, dimensionless
n = reaction order for noncatalytic reaction, dimensionless
P_a = equilibrium adsorption pressure
P_o = saturation vapor pressure at adsorption temperature
R = particle radius, m
R_o = R at $t = 0$, m
S_o = total surface area per unit volume of unreacted particle, m^2/m^3
t = reaction time, s
V_b = bulk solid volume per unit weight of particls, m^2/g
V_s = volume of the catalyst solution, m^3
V_T = total pore volume per unit weight of sample, m^3/g
V_t = true solid volume per unit weight of particles, excluding pore volume, m^3/g
X = conversion, dimensionless

Greek Letters

α = ratio of catalytic to noncatalytic reaction rates
ϵ = porosity, dimensionless
ϵ_o = initial porosity, dimensionless
ρ_b = bulk density of solid particles, g/cm^3
ρ_t = true density of solid particles, excluding pore volume, g/cm^3
σ = $R_o S_o/(1-\epsilon_o)$, a particle size parameter
τ = $k_s C_o t S_o (1-\epsilon_o)$, dimensionless time
ψ = $4\pi L_o(1-\epsilon_o)/S_o^2$, a pore structure parameter
Ω = ratio of catalytic to noncatalytic contributions to overall reaction rate

LITERATURE CITED

Adam, N. K., and G. E. P. Elliott, "Contact Angles of Water against Saturated Hydrocarbons," *J. Chem. Soc.*, 2,206 (1952).

Bhatia, S. K., and D. D. Perlmutter, "A Random Pore Model for Fluid-Solid Reactions. I: Isothermal, Kinetic Control," *AIChE J.*, **26**, 379 (1980).

Gan, H., S. P. Nandi, and P. L. Walker, Jr., "Nature of the Porosity in American Coals," *Fuel*, **51**, 272 (1972).

Haggin, J., "Interest in Coal Chemistry Intensifies," *Chem. Eng. News*, 17, (Aug. 9, 1982).

Hartstein, A. M., R. W. Freedman, and D. Platter, "Novel Wet-Digestion Procedure for Trace-Metal Analysis of Coal by Atomic Absorption," *Anal. Chem.*, **45**, 611 (1973).

Hirsch, R., et al., "Catalytic Coal Gasification: An Emerging Technology," *Science*, **215**, 121 (1982).

Huhn, F., J. Klein, and H. Jüntgen, "Investigations on the Alkali-Catalyzed Steam Gasification of Coal: Kinetics and Interactions of Alkali Catalyst with Carbon," *Fuel*, **62**, 196 (1983).

Ingles, O. G., "The Contact Angle of Mercury at Coal and Char Surfaces," *Fuel*, **36**, 252 (1957).

Johnson, J. L., "The Use of Catalysts in Coal Gasification," *Catal. Rev. Sci. Eng.*, **14**(1), 131 (1976).

Lang, R. J., and R. C. Neavel, "Behavior of Calcium as a Steam Gasification Catalyst," *Fuel*, **61**, 620 (1982).

McKee, D. W., "The Catalyzed Fasification Reactions of Carbon," *Chemistry and Physics of Carbon*, **16**, 1, Marcel Dekker, New York (1981).

McKee, D. W., et al., "Catalysis of Coal Char Gasification by Alkali Metal Salts," *Fuel*, **62**, 217 (1983).

Otto, K., and M. Shelef, "Catalytic Steam Gasification of Carbons: Effect of Ni and K on Specific Rates," *Proc. 6th Int. Cong. on Catal.*, **2**, 1,082, The Chemical Society, Burlington House, London (1976).

Patrick, J. W., and F. H. Shaw, "Influence of Sodium Carbonate on Coke Reactivity," *Fuel*, **51**, 69 (1972).

Prasher, B. D., "An Assessment of Catalytic Gasification," Morgantown Energy Technology Center, U.S. Dept. of Energy," Report METC/SP-79/7 (Jan., 1979).

Schrader, M. E., "Ultrahigh Vacuum Techniques in the Measurement of Contact Angles. IV: Water on Graphite (0001)," *J. Phy. Chem.* **79**(23), 2,508 (1975).

Senkan, S., and E. L. Fuller, Jr., "Effect of NaOH Treatment on Surface Properties of Coal," *Fuel*, **58**, 731 (1979).

Spackman, W., et al., "Evaluation and Development of Special Purpose Coals," Fossil Energy, Coal Res. Sec., Penn. State Univ., (Sept. 1976).

Spiro, C. L., et al., "Catalytic CO_2-Gasification of Graphite vs. Coal Char," *Fuel*, **62**, 180 (1983).

Su, J. L., "Pore Structure and Catalyst Effects on Char Gasification Kinetics," Ph.D. Thesis, Univ. of Pennsylvania (1983).

Taylor, H. S., and H. A. Neville, "Catalysis in the Interaction of Carbon with Steam and with Carbon Dioxide," *J. Amer. Chem. Soc.*, **43**, 2,055 (1921).

Trupathi, V. S., and P. K. Ramachandran, "Studies on Metal Impregnated Activated Carbon: Complete Pore Structure Analysis," *Carbon*, **20**, 25 (1982).

Vargas, J., "Kinetics and Physical Changes During the Pyrolysis of Bituminous Coal," Ph.D. Thesis, Univ. of Pennsylvania (1982).

Veraa, M. J., and A. T. Bell, "Effect of Alkali Metal Catalysts on Gasification of Coal Char," *Fuel*, **57**, 194 (1978).

Walker, Jr., P. L., M. Shelef, and R. A. Anderson, "Catalysis of Carbon Gasification," *Chemistry and Physics of Carbon*, **2**, 287, Marcel Dekker, New York (1966).

Walker, Jr., P. L., et al., "Catalysis of Gasification of Coal-Derived Cokes and Chars," *Fuel*, **62**, 140 (1983).

Wen, W. Y., "Mechanisms of Alkali Metal Catalysis in the Gasifications of Coal, Char, or Graphite," *Catal. Rev. Sci. Eng.*, **22**(1), 1 (1980).

Wigmans, T., J. Van Doorn, and J. A. Moulign, "Temperature-Programmed Desorption Study of Na_2CO_3-Containing Activated Carbon," *Fuel*, **62**, 190 (1983a).

Wigmans, T., H. Haringa, and J. A. Moulijn, "Nature, Activity and Stability of Active Sites during Alkali Metal Carbonate-Catalyzed Gasification Reactions of Coal Char," *Fuel*, **62**, 185 (1983b).

Wigmans, T., et al., "The Influences of Potassium Carbonate on Surface Area Development and Reactivity During Gasification of Activated Carbon by Carbon Dioxide," *Carbon*, **21**, 113 (1983c).

Yuh, S. J., and E. E. Wolf, "FTIR Studies of Potassium Catalyst-Treated Gasified Coal Chars and Carbons," *Fuel*, **62**, 252 (1983).

Manuscript received Apr. 3, 1984; revision received Oct. 4, and accepted Oct. 15.